Anti-inflammatory apoA-I-mimetic peptides bind oxidized lipids with much higher affinity than human apoA-I

Brian J. Van Lenten,[1,*] Alan C. Wagner,[*] Chun-Ling Jung,[*] Piotr Ruchala,[*] Alan J. Waring,[*] Robert I. Lehrer,[*] Andrew D. Watson,[*] Susan Hama,[*] Mohamad Navab,[*] G. M. Anantharamaiah,[†] and Alan M. Fogelman[*]

Department of Medicine* David Geffen School of Medicine, University of California Los Angeles, Los Angeles, CA 90095-1679; and The Atherosclerosis Research Unit,[†] Department of Medicine, University of Alabama at Birmingham, Birmingham, AL 35294

Abstract **4F is an anti-inflammatory, apolipoprotein A-I (apoA-I)-mimetic peptide that is active in vivo at nanomolar concentrations in the presence of a large molar excess of apoA-I. Physiologic concentrations (~35 μM) of human apoA-I did not inhibit the production of LDL-induced monocyte chemotactic activity by human aortic endothelial cell cultures, but adding nanomolar concentrations of 4F in the presence of ~35 μM apoA-I significantly reduced this inflammatory response. We analyzed lipid binding by surface plasmon resonance. The anti-inflammatory 4F peptide bound oxidized lipids with much higher affinity than did apoA-I. Initially, we examined the binding of PAPC (1-palmitoyl-2-arachidonoyl-*sn*-glycero-3-phosphatidylcholine) and observed that its oxidized products bound 4F with an affinity that was ~4–6 orders of magnitude higher than that of apoA-I. This high binding affinity was confirmed in studies with defined lipids and phospholipids. 3F-2 and $3F^{14}$ are also amphipathic α-helical octadecapeptides, but 3F-2 inhibits atherosclerosis in mice and $3F^{14}$ does not. Like 4F, 3F-2 also bound oxidized phospholipids with very high affinity, whereas $3F^{14}$ resembled apoA-I. The extraordinary ability of 4F to bind pro-inflammatory oxidized lipids probably accounts for its remarkable anti-inflammatory properties.**—Van Lenten, B. J., A. C. Wagner, C-L. Jung, P. Ruchala, A. J. Waring, R. I. Lehrer, A. D. Watson, S. Hama, M. Navab, G. M. Anantharamaiah, and A. M. Fogelman. **Anti-inflammatory apoA-I-mimetic peptides bind oxidized lipids with much higher affinity than human apoA-I.** ***J. Lipid Res.*** **2008.** 49: **2302–2311.**

Supplementary key words atherosclerosis • apolipoprotein A-I • lipoproteins • oxidized phospholipids

The 4F peptides L-4F and D-4F are apolipoprotein A-I (apoA-I) mimetics that demonstrate prominent anti-inflammatory properties in vitro and in animal models (1–22). ApoA-I has a mass of 28 kDa, and is present in human and mouse plasma at a concentration of ~35 μM. D-4F is a 2.3 kDa peptide, and after oral administration of D-4F to mice, its maximal plasma concentration was only ~130 nM (7). Humans who received a single oral dose of D-4F had even lower plasma concentrations, ~4 nM (23). Despite such low levels, HDL isolated from mice or humans that had received a single dose of D-4F became significantly more "anti-inflammatory," as judged by the diminished monocyte chemotactic activity generated by human aortic endothelial cells (HAECs) treated with LDL. This anti-inflammatory effect was also demonstrated in vitro, inasmuch as adding ~120 nM 4F to the plasma of selected human patients containing ~35 μM apoA-I also reversed the pro-inflammatory properties of their HDL (24). In other in vitro experiments, we added D-4F to apoE-null mouse plasma. When such plasma was fractionated by fast-protein liquid chromatography, we noted the movement of 15-hydroxyeicosatetraenoic acid (15-HETE) into the fractions containing D-4F (7), suggesting that the affinity of D-4F for this oxidized lipid might be much greater than that of apoA-I.

Consistent with this hypothesis was the finding that adding human apoA-I to human artery wall cells in a preincubation followed by removal of the apoA-I prior to the addition of human LDL dramatically reduced the ability of the cells to oxidize LDL to a form that could stimulate the induction of monocyte chemoattractant protein-1 (MCP-1) as determined by a bioassay (25). However, if the apoA-I was left in the cultures when the LDL was added (a coincubation) the oxidation of LDL and the induction of MCP-1 was the same as if the apoA-I had not been added (25). In contrast, the addition of D-4F prevented LDL oxidation and MCP-1 induction even in a co-

This work was supported in part by US Public Health Service Grants HL-30568 and HL-34343 and the Laubisch, Castera, and M. K. Grey Funds at UCLA. MN, SH, GMA and AMF are principals in Bruin Pharma and AMF is an officer in Bruin Pharma.

Manuscript received 11 February 2008 and in revised form 24 June 2008 and in re-revised form 10 July 2008.

Published, JLR Papers in Press, July 11, 2008.
DOI 10.1194/jlr.M800075-JLR200

Abbreviations: apoA-I, apolipoprotein A-I; HAEC, human aortic endothelial cell; MCP-1, monocyte chemoattractant protein-1; RU, resonance unit; SPR, surface plasmon resonance; SREBP, sterol-regulatory element binding protein.

[1] To whom correspondence should be addressed.
e-mail: bvanlent@mednet.ucla.edu

incubation (1). We hypothesized that apoA-I bound the oxidized lipids with lower affinity, compared with D-4F, allowing the lipids to dissociate from the apoA-I and stimulate MCP-1 production. In contrast, the affinity of oxidized lipids for D-4F was postulated to be so strong that they could not effectively dissociate and MCP-1 production was prevented (24).

The specificity of 4F for oxidized lipids was also suggested by recent in vivo studies. D-4F treatment dramatically reduced the levels of oxidized lipids recognized by the monoclonal antibody EO6 in kidney tissue without significantly affecting renal apoB, plasma lipid, or plasma lipoprotein levels (22).

In the studies reported here, we used surface plasmon resonance (SPR) measurements to compare the binding of nonoxidized lipids and oxidized lipids to full-length human apoA-I and to apoA-I-mimetic peptides. The results indicate that specific mimetic peptides have an increased binding affinity for oxidized phospholipids, compared with the parent nonoxidized phospholipids, whereas full-length human apoA-I binds oxidized and nonoxidized phospholipids similarly. The mimetic peptides bind oxidized and nonoxidized FAs with similar high affinity, whereas full-length human apoA-I binds oxidized FAs with a much lower affinity, compared with the nonoxidized parent FAs. We also directly tested the ability of an apoA-I-mimetic peptide (4F) to inhibit LDL induction of MCP-1 in cultures of HAECs incubated in the presence of a vast excess of human apoA-I, and we found that 4F (but not apoA-I) was highly effective in preventing LDL induction of MCP-1 under these conditions.

MATERIALS AND METHODS

Lipids

PAPC (L-α-1-palmitoyl-2-arachidonoyl-*sn*-glycero-3-phosphorylcholine), PAPE (1-palmitoyl-2-arachidonoyl-*sn*-glycero-3-phosphatidylethanolamine), POVPC (1-palmitoyl-2-(5-oxovaleroyl)-*sn*-glycero-3-phosphorylcholine, and PGPC (1-palmitoyl-2-glutaroyl-*sn*-glycero-3-phosphorylcholine), were from Avanti Polar Lipids (Alabaster, AL). Cholesterol, ≥99% pure, 20(*S*)-hydroxycholesterol, 22(*S*)- and 25-hydroxycholesterol, arachidonic acid, linoleic acid, palmitic acid, hexanonic acid, octanoic acid, decanoic acid, and glycerol trioleate were from Sigma-Aldrich (St. Louis, MO). 13(*S*)-HPODE (hydroperoxyoctadecadienoic acid), 5(*S*)-, 12(*S*)-, and 15(*S*)-HPETE (hydroperoxyeicosatetraenoic acid), 12(*S*)- and 15(*S*)-HETE (hydroperoxyoctadecadienoic acid), were from BioMol, Plymouth Meeting, PA. 9(*S*)-, 13(*S*)-HODE (hydroxyoctadecadienoic acid) and KOdiA-PC (1-palmitoyl-2-(5-keto-6-octenedioyl)-*sn*-glycero-phosphatidylcholine) (26) were from Cayman Chemical US (Ann Arbor, MI), and 4-β- and 24(*S*)-hydroxycholesterol were from Steraloids (Newport, RI). Air-oxidized PAPC (oxPAPC) and PEIPC (1-palmitoyl-2-(5,6-eoxyisoprostane E2)-*sn*-glycero-3-phosphorylcholine) were prepared as previously described (27, 28).

Peptides and proteins

D-4F and L-4F (Ac-DWFKAFYDKVAEKFKEAF-NH_2) have the same sequence, but are enantiomers, with one (D-4F) composed exclusively of D-amino acids and the other containing only L-amino acids. The inactive control peptide called Scrambled L-4F (ScL-4F) has the same overall amino acid composition as L-4F but in a sequence that does not promote amphipathic α-helix formation (Ac-DWFAKDYFKKAFVEEFAK-NH_2). These three peptides were synthesized as previously described (1), as were 3F-2 (Ac-DKWKAVYDKFAEAFKEFL-NH_2) and $3F^{14}$ (Ac-DWLKAFYDK-VAEKFKEAF-NH_2) (29, 30). The synthesis of N-terminally biotinylated L-4F was done on a Symphony automated peptide synthesizer (Protein Technologies, Inc., Tucson, AZ), using conventional 9-fluorenylmethoxycarbonyl (Fmoc) chemistry (31) and commercially available amino acid derivatives and reagents (EMD Biosciences, San Diego, CA). Biotin (Pierce, Rockford, IL) was introduced via the flexible 6-aminohexanoic linker (Ahx). The biotinylated peptide (Biotin-Ahx-D-WFKAFYDKVAEKFKEAF-NH_2) was cleaved from the resin by applying a mixture of trifluoracetic acid (94% v/v), phenol (2% w/v), water (2% v/v), and triisopropysilane (2% v/v) for 2 h. The peptide was precipitated with ice-cold diethyl ether and purified by preparative reverse-phase (RP)-HPLC) to >95% homogeneity by analytical RP-HPLC and matrix-assisted laser desorption ionization-mass spectrometry. Purified human apoA-I (purity approximately 97%) was purchased from Sigma-Aldrich, and purified human apoA-I "Cappel brand" (purity >98%) was purchased from MP Biomedicals (Solon, OH), and these were used interchangeably because the two preparations gave similar results. BSA was from Sigma-Aldrich.

Binding studies

Binding studies were performed by SPR on a BIAcore 3000 system (BiaCore AB, Piscataway, NJ). In most experiments, peptide ligands and apoA-I were immobilized on a BIAcore CM5 sensor chip activated per the manufacturer's protocol with *N*-hydroxysuccinimide and 1-ethyl-3-(3-dimethylaminoisopropyl) carbodiimide. After achieving adequate immobilization, the sensor surface was deactivated with ethanolamine. Analyte solutions were prepared in a standard BIAcore buffer (HBS-EP), containing 10 mM HEPES, pH 7.4, 150 mM NaCl, 3 mM EDTA, and 0.005% (v/v) surfactant P20. Lipid stock solutions were prepared in ethanol, so that analyte-containing, HBS-EP binding buffer contained up to 2.0% ethanol. Lipid binding was measured by observing the change in the SPR angle as 30 μl of lipid (various concentrations) in HBS-EP buffer flowed over the sample for 3 min at 10 μl/min. The chip was regenerated between trials by washing with 25% or 50% ethanol. Equilibrium affinity constant (K_D) values were calculated from assays performed with five different lipid concentrations that gave binding responses of 30 to >500 resonance units (RUs). The calculations were done with BIAcore's BIAevaluation software, version 4.1, assuming a molar ratio of 1:1 lipid:protein binding. For oxidized PAPC, such calculations necessarily assumed that a single phospholipid species of known molecular weight was present, whereas in reality, multiple oxidized species of different masses were present. We identify any such K_D values as K_{Dapp} (apparent K_D values) to emphasize their qualitative nature, as is further discussed below. To remedy this, experiments with oxidized PAPC were repeated with well-defined lipids, including several previously identified components of the oxidized PAPC preparation (32, 33). Given the difference in the mass of the peptides relative to the mass of apoA-I, in an attempt to equalize the molar densities of these ligands, the biosensors contained 4- to 6-fold more RUs of immobilized apoA-I than 4F, and the apoA-I result was scaled and normalized by multiplying the observed binding to equalize the relative molar densities of the apoA-I and 4F on the biosensors.

N-biotinylation

The aforementioned procedure attaches sensing molecules to the sensor chip by converting one or more of their amino groups

into peptide bonds. For most peptides and proteins, this can be either the N-terminal amino group or the ε-amino group of one or more lysine residues. Because the various apoA-mimetic peptides had blocked N-termini, only the latter mode of coupling applied. To address the possibility that having different or multiple lysines as attachment sites might vary the conformations of the immobilized proteins and peptides, we performed some binding studies with N-biotinylated L-4F that was affixed to a streptavidin (Sigma-Aldrich)-coated BIAcore SA chip to provide a biosensor containing L-4F with unmodified lysine residues. This approach allowed us to use freely mobile peptides in completely native conformations. In addition, we tested the converse situation by preparing a biotinylated analog of the phospholipid PAPE. Briefly, biotin was linked to ethanolamine at the *sn*-3 position of PAPE in the presence of dicyclohexylcarbodiimide and dimethylaminopyridine in dichloromethane as previously described (34). PAPE-*N*-Biotin was purified by preparative HPLC and then oxidized in air (usually 48–72 h). The oxidized and nonoxidized lipids were bound to BIAcore SA chips so that the acyl chains in the *sn*-1 and *sn*-2 positions were presumably freely mobile in the solvent.

Cell culture and other methods

HAECs were cultured as previously described (21). The production of MCP-1 was measured by bioassay as monocyte chemotactic activity as described (25) and normalized to the levels induced by LDL alone (21). Other methods, including statistical analyses were as described (21).

RESULTS

We previously reported that adding 50 μg/ml of human apoA-I to human artery wall cells in culture did not prevent LDL oxidation and induction of MCP-1 as measured by a bioassay if the apoA-I was added at the same time as LDL (25). As shown in **Fig. 1**, adding 1 mg/ml (~35 μM) of human apoA-I to HAECs did not decrease LDL-induced monocyte chemotactic activity and actually slightly increased it. In the experiments shown in Fig. 1, L-4F was added at concentrations ranging from 0.43 nM (0.001 μg/ml) to 0.43 μM (1 μg/ml) in the presence of 35 μM (1 mg/ml) of human apoA-I. At a concentration of 4.3 nM (0.01 μg/ml), L-4F significantly ($P < 0.001$) decreased the LDL-induced monocyte chemotactic activity, and 0.43 μM of L-4F reduced the levels to those achieved with normal human HDL (Fig. 1). The effect of L-4F on the lipoprotein inflammatory index in the absence of apoA-I was not significantly different at any concentration tested, compared with L-4F in the presence of apoA-I (data not shown). Thus, the effect of L-4F did not depend on the presence of full-length apoA-I. These results confirm and extend our previous results (25) and directly prove that 4F is effective at nanomolar concentrations even in the presence of a very large excess of human apoA-I.

Figure 2 shows the effects of oxidizing PAPC on its binding to apoA-I and the 4F peptides. The total duration of oxidation was 48 h, and during that time, PAPC was converted to multiple different components, collectively designated "oxPAPC." At the conclusion of oxidation, no intact PAPC was observed by mass spectrometry (data not shown).

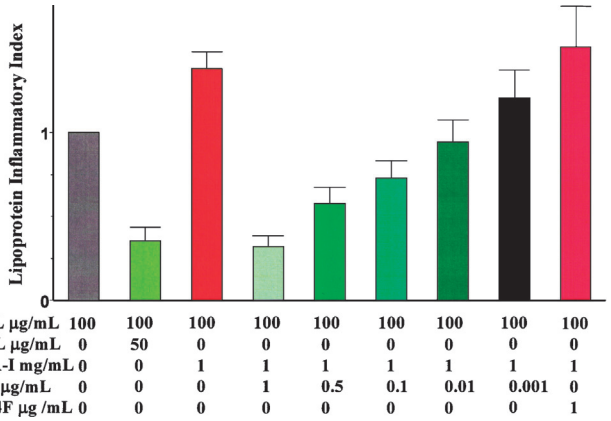

Fig. 1. L-4F, but not apolipoprotein A-I (apoA-I), inhibits LDL-induced monocyte chemotactic activity in cultures of human aortic endothelial cells (HAECs). Human LDL (hLDL) was added to cultures of HAECs with or without hHDL or full-length human apoA-I, or L-4F added together with the apoA-I at the concentrations shown. As a control, apoA-I was also added with an inactive form of L-4F, scrambled 4F (ScL-4F), and monocyte chemotactic activity was determined and normalized to LDL alone, as described in Materials and Methods. Statistical analysis: $P < 0.001$, hHDL + hLDL versus hLDL alone; $P < 0.001$, apoA-I + hLDL versus LDL alone; $P < 0.001$, apoA-I + L-4F (1 μg/ml) + hLDL versus apoA-I + hLDL; $P < 0.001$, apoA-I + L-4F (0.5 μg/ml) + hLDL versus apoA-I + hLDL; $P < 0.001$, apoA-I + L-4F (0.1 μg/ml) + hLDL versus apoA-I + hLDL; $P < 0.001$, apoA-I + L-4F (0.01 μg/ml) + hLDL versus apoA-I + hLDL; $P > 0.05$, apoA-I + L-4F (0.001 μg/ml) + hLDL versus apoA-I + hLDL; $P > 0.05$, apoA-I + ScL-4F (1 μg/ml) + hLDL versus apoA-I + hLDL. The values shown are the mean ± SD from quadruplicate determinations for a total of 36 high-powered fields examined in each experiment (n=3).

Samples of oxPAPC were removed and tested at intervals, and the "apparent *K*" (K_{Dapp}) values were calculated. The K_{Dapp} of oxidized PAPC for binding apoA-I changed very little, whereas for D-4F and L-4F, it decreased by several orders of magnitude (Fig. 2A). Even at the zero-hour time point, the binding isotherms of apoA-I and the 4F peptides differed substantially when concentrations well below the K_{Dapp} were tested (Fig. 2B). Similar behavior was also seen when subsequent oxPAPC samples were tested (Fig. 2C, D).

When comparing K_D data with a binding isotherm, it must be recalled that the K_D value is derived from the equation: $K_D = k_d/k_a$. In this equation, k_d represents the dissociation rate constant and has units of 1/sec, and k_a represents the association rate constant and has units of 1/Msec. The high affinity (low K_D value) of the oxPAPC preparations derives principally from their much higher association rates, which are reflected in the isotherms by the much steeper upward slope of the binding curves for the 4F peptides. In Fig. 2, the k_a values for oxPAPC were 9.92×10^6/Msec, 9.04×10^6/Msec, and 6.41×10^3/Msec for L-4F, D-4F, and apoA-I, respectively, whereas for PAPC, the k_a values were 1.22×10^3/Msec, 1.12×10^3/Msec, and 319/Msec for L-4F, D-4F, and apoA-I, respectively.

We used homogeneous lipid preparations to further evaluate the binding of oxidized lipids by the 4F peptides. **Table 1** shows the affinity of four pro-inflammatory oxi-

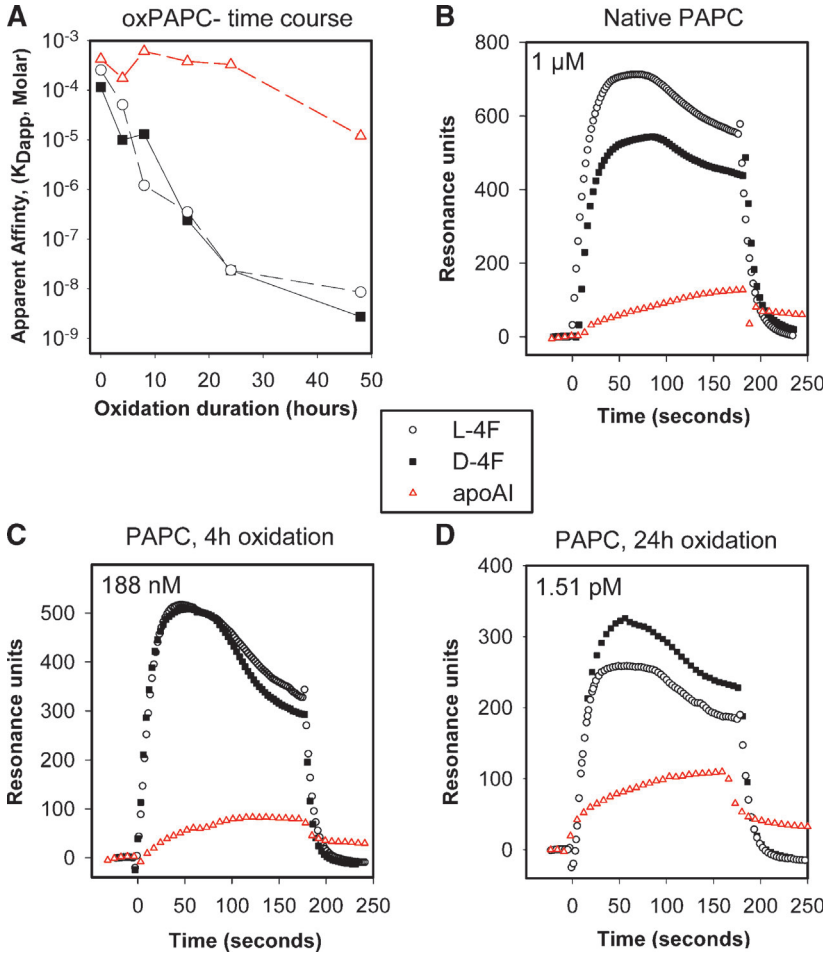

Fig. 2. Binding of PAPC and oxPAPC. PAPC was incubated in air for up to 48 h to generate oxPAPC, and its binding was compared with native PAPC initially. A: "Apparent K_D "(K_{Dapp}) values for D-4F, L-4F, and apoA-I for samples removed at intervals during the oxidation. The binding isotherms show selected phospholipid concentrations tested at zero-time (B), after 4 h of PAPC oxidation (C), and after 24 h of PAPC oxidation (D), and are discussed in the text. Biosensors contained 1,045 resonance units (RUs) of L-4F, 996 RUs of D-4F, and 5,743 RUs of apoA-I. The apoA-I result was scaled and normalized by multiplying the observed binding by 2.148, to equalize the relative molar densities of the apoA-I and 4F on the biosensors.

dized phospholipids for D-4F, L-4F, and apoA-I. On average, the 4F peptides had K_D values that were about 3,000-fold lower than those of apoA-I. For PEIPC, one of the most bioactive pro-inflammatory phospholipids (26), D-4F had a K_D of 0.064 nM, L-4F had a K_D of 0.01 nM, and apoA-I had a K_D of 50 μM, a difference of about six orders of magnitude.

Several nonoxidized FFAs that varied in chain length and saturation were bound with equal affinity by apoA-I, D-4F, and L-4F (**Table 2**). However, oxidized species such as HPETE (hydroperoxyeicosatetraenoic acid), HPODE (hydroperoxyoctadecadienoic acid), HETE (hydroxyeicosatetraenoic acid), and HODE (hydroxyoctadecadienoic acid) were bound with K_D values that were often five orders of magnitude lower for 4F peptides than for apoA-I (Table 2). This difference resulted because the K_D values for binding to the peptides were similar for the oxidized FAs and their nonoxidized precursors. In contrast, these oxidized FAs bound apoA-I with much lower affinity than their nonoxidized precursors. **Figure 3** shows binding curves for eight concentrations of one of these oxidized lipids, 13(*S*)-HPODE: 1.5, 2.0, 3.0, and 5.0 μg/ml (~4.8, 6.4, 9.7, and 16.1 μM) and 30, 40, 50 and 90 ng/ml (~97, 129, 161, and 290 nM). At the higher concentrations, L-4F had a K_D of 16.8 ± 4.3 nM. The corresponding K_D for apoA-I was 1.23 ± 0.57 mM. Native and oxidized cholesterol also bound to the mimetic peptides with substantially higher affinity than to apoA-I (**Table 3**). Neither cholesterol nor its oxidized analogs bound sufficiently to apoA-I for us to estimate a K_D.

In the experiments described above, the lipids were not associated with lipoproteins. To determine whether lipids associated with lipoproteins would behave similarly, the binding of LDL that had been incubated overnight with HAECs was compared with the binding of LDL that was not incubated with HAECs. We have previously reported that incubating LDL with HAECs results in the transfer of hydroperoxy FAs such as HPODE from the endothelial cells to LDL (25). The binding affinity (K_D) of LDL that had

TABLE 1. Affinity of specific oxPAPC components for D-4F, L-4F, and apoA-I

Lipids	K_D		
	D-4F	L-4F	apoA-I
	nM		
PAPC	118,576 ± 36,843	192,821 ± 56,505	99,871 ± 14,114
PGPC	6.3 ± 4.2	7.2 ± 4.5	4,206 ± 4,228
POVPC	2.4 ± 2.0	3.6 ± 2.6	30,852 ± 28,314
PEIPC	0.06 ± 0.05	0.01 ± 0.01	50,720 ± 5,721
KOdiA-PC	0.58 ± 0.0	1.58 ± 3.5	20,960 ± 11,680

apoA-I, apolipoprotein A-I; PAPC, 1-palmitoyl-2-arachidonoyl-sn-glycero-3-phosphorylcholine; PGPC, 1-palmitoyl-2-glutaroyl-*sn*-glycero-3-phosphorylcholine; POVPC, 1-palmitoyl-2-(5-oxovaleroyl)-*sn*-glycero-3-phosphorylcholine; PEIPC, 1-palmitoyl-2-(5,6-epoxyisoprostane E2)-*sn*-glycero-3-phosphorylcholine; KOdiA-PC, 1-palmitoyl-2-(5-keto-6-octenedioyl)-*sn*-glycero-phosphatidylcholine. Binding was determined by surface plasmon resonance (SPR), as described in Materials and Methods. The values shown are the mean ± SEM from five separate experiments.

been incubated with HAECs was not different from the binding affinity of native LDL for human apoA-I (K_D = 167 ± 27 nM vs. 137 ± 16 nM). In contrast, the binding affinity of LDL that had been incubated with HAECs was increased by 6.1-fold, compared with the binding affinity of native LDL for L-4F (K_D = 141 ± 32 nM vs. 23 ± 9 nM; $P < 0.001$). Adding 13(*S*)-HPODE to native LDL (500 ng 13(*S*)-HPODE incubated with 50 μg LDL/ml for 2 h at 37°C) resulted in a dramatic increase in the binding affinity of LDL for L-4F (K_D = 0.42 nM; $P < 0.0079$) but did not result in a significant change in the binding affinity of LDL for apoA-I.

In the examples shown up to this point, apoA-I and the N-terminally blocked apoA-I-mimetic 4F peptides were immobilized to the sensor chip by an amine-coupling procedure that converted one or more of their lysine-ε-amino group(s) into one or more amides. To assure ourselves that this immobilization procedure had not somehow enhanced the ability of the 4F peptides to bind oxidized lipids, binding studies were also performed by attaching N-biotinylated L-4F to a streptavidin-coated CM5 chip. Using results obtained with a series of phospholipid concentrations, we calculated a K_{Dapp} value of 3.1×10^{-8} M for oxPAPC and a K_D of 2.2×10^{-4} M for native PAPC. **Figure 4A** shows studies done with two concentrations of native PAPC and oxPAPC: 1 μM and 1 pM. Immobilized biotinylated L-4F bound both at the 1 μM concentration, but bound only oxPAPC at the 1 pM level. Figure 4B shows that immobilized biotinylated L-4F could even bind subpicomolar (attomolar) concentrations of KOdiA-PC. In other studies, it was determined that the biotinylation of L-4F did not alter its biologic activity (data not shown).

As a further control, we reversed the binding conditions by immobilizing the lipid on the sensor chip and introducing the 4F peptides in solution. To do so, we biotinylated 1-palmitoyl-2-arachidonoyl-*sn*-glycero-3-phosphatidylethanolamine (PAPE) to prepare PAPE-*N*-Biotin. Whereas one aliquot of this reagent was stored under argon at −80°C, another was allowed to oxidize for 48–72 h (as monitored by electrospray ionization-mass spectrometry) to prepare oxPAPE-*N*-Biotin as described in Materials and Methods, and then both were coupled to streptavidin-coated sensor chips. Where as little as 60 femtograms of L-4F/ml (~26 fM) gave a good binding signal with immobilized *N*-biotin-oxPAPE (**Fig. 5**), even 100 μg/ml of L-4F (43.3 μM) failed to bind immobilized PAPE-*N*-Biotin that had not been oxidized. The apparent affinity of soluble L-4F for immobilized oxPAPE-*N*-Biotin (K_{Dapp} = 1.36×10^{-9} M) was similar, and perhaps greater than its affinity

TABLE 2. Affinity of oxidized and nonoxidized lipids for D-4F, L-4F, and apoA-I

Ligands	K_D		
	D-4F	L-4F	apoA-I
		nM	
Nonoxidized lipids			
Arachidonic acid	12.2 ± 1	15.0 ± 1.3	10.5 ± 1.5
Linoleic acid	14.78 ± 1.58	11.73 ± 3.5	6.55 ± 2.53
Hexanoic acid	208 ± 39	470 ± 156	908 ± 328
Octanoic acid	28,660 ± 4,887	27,368 ± 12,461	44,420 ± 10,461
Decanoic acid	297,760 ± 79,252	260,800 ± 54,130	269,000 ± 62,475
Oxidized lipids			
5(*S*)-HPETE	178.3 ± 70.6	91.7 ± 15.6	1,582,000 ± 349,648
12(*S*)-HPETE	169 ± 125	98.3 ± 34.2	822,600 ± 266,325
15(*S*)-HPETE	51.5 ± 13.5	51.8 ± 11	1,046,400 ± 160,782
13(*S*)-HPODE	20.7 ± 5.3	16.8 ± 4.3	1,230,800 ± 569,295
12(*S*)-HETE	18.4 ± 5.5	23.4 ± 7	849,600 ± 327,395
15(*S*)-HETE	22.3 ± 7.7	21 ± 6.8	1,289,400 ± 139,245
9(*S*)-HODE	15 ± 3.8	25.8 ± 10.6	1,312,200 ± 534,323
13(*S*)-HODE	20.8 ± 6	31.8 ± 3.7	1,803,400 ± 279,731
Controls			
Glycerol trioleate	408 ± 84	310 ± 55	224 ± 122
Bovine albumin	3,932 ± 1,526	7,520 ± 3,888	21.1 ± 4.5

HPETE, hydroperoxyeicosatetraenoic acid; HPODE, hydroperoxyoctadecadienoic acid, HETE, hydroxyeicosatetraenoic acid; HODE, hydroxyoctadecadienoic acid. Binding was determined by SPR, as described in Materials and Methods. The values shown are the mean ± SEM from five separate experiments.

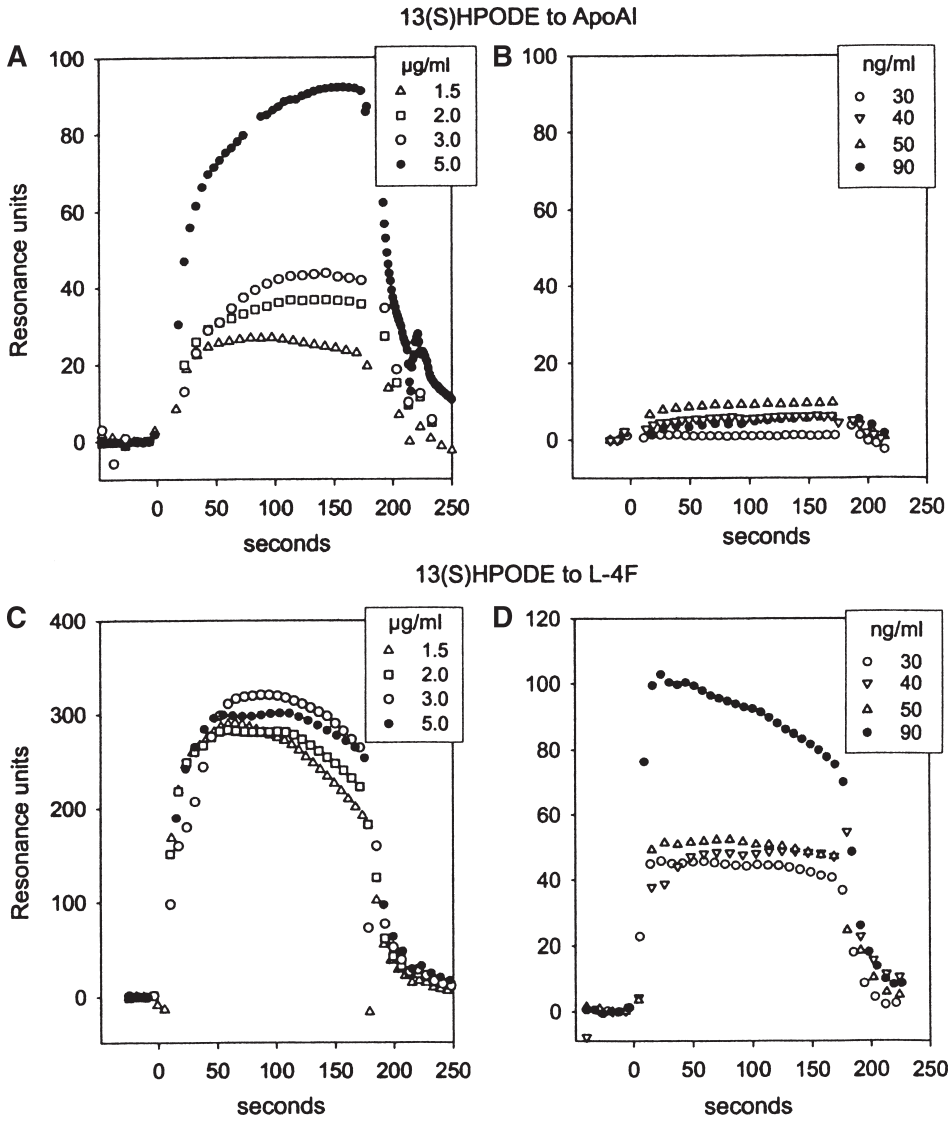

Fig. 3. Binding of 13(*S*)-HPODE to apoA-I and L-4F. These binding curves are representative of those used to compute the K_D data for the various lipids in Tables 1 and 2. A: Binding of high concentrations of 13(*S*)-HPODE to apoA-I. B: Binding of low concentrations of 13(*S*)-HPODE to apoA-I. C: Binding of high concentrations of 13(*S*)-HPODE to L-4F. D: Binding of low concentrations of 13(*S*)-HPODE to L-4F. The biosensors contained 706 RU of L-4F and 3,299 RU of apoA-I. The observed apoA-I binding was scaled to equalize the relative molar densities of apoA-I and 4F on the biosensors.

when the L-4F was biotinylated and immobilized to the biosensor and the unmodified lipids were in solution.

Whereas apoA-I contains 243 amino acid residues, the apoA-I-mimetic peptides contain only 18 amino acids. Accordingly, we tested two additional 18-residue apoA-I-mimetic peptide analogs, 3F-2 and 3F[14]. Although both have class A, amphipathic helical structures and they bind nonoxidized lipids similarly, 3F-2 inhibited atherosclerotic lesion formation in a mouse model and 3F[14] did not (30). **Figure 6A** shows that immobilized 3F-2 and L-4F bound oxPAPC identically; however its binding by 3F[14] was significantly less, resembling its binding by apoA-I (Fig. 2A). Moreover, when 3F-2 and 3F[14] were compared for their ability to bind specific oxPAPC components (POVPC, PGPC, and PEIPC) as well as the oxidized lipid 15(*S*)-HPETE, 3F-2 was more effective (Fig. 6B). Thus, the anti-inflammatory peptides 3F-2 and 4F bind pro-inflammatory oxidized lipids and phospholipids with an affinity that is much higher than that shown by apoA-I or by 3F[14].

DISCUSSION

We previously reported that human apoA-I was significantly more potent than mouse apoA-I in rendering HDL anti-inflammatory in a mouse model of atherosclerosis (35). In other studies, we reported that the apoA-I-mimetic peptide D-4F was much more anti-inflammatory than human apoA-I in LDL receptor-null mice with influenza A viral pneumonia (3). The data reported here indicate that the binding affinities for nonoxidized phospholipids are similar for human apoA-I and the mimetic peptides D-4F,

TABLE 3. Affinity of sterols for D-4F, L-4F, and apoA-I

Sterols	K_D		
	D-4F	L-4F	apoA-I
	nM		
Cholesterol	91.84 ± 28	11.6 ± 3	BND
20(*S*)-hydroxycholesterol	3,953 ± 2,125	243 ± 53	BND
22(*S*)-hydroxycholesterol	14,662 ± 4,338	11,623 ± 5,631	BND
24(*S*)-hydroxycholesterol	4,356 ± 1,654	1,326 ± 393	BND
25-hydroxycholesterol	2,375 ± 1,556	983 ± 431	BND
4β-hydroxycholesterol	30,608 ± 16,996	10,898 ± 6,472	BND

BND, binding not detected. Binding was determined by SPR, as described in Materials and Methods. The values shown are the mean ± SEM from five separate experiments.

L-4F, 3F-2, and $3F^{14}$. Oxidation of PAPC only minimally changed the binding affinity for apoA-I and $3F^{14}$ (a biologically inactive peptide). In contrast, the binding affinities of oxPAPC and defined oxidized phospholipids for D-4F, L-4F, and 3F-2 (peptides that inhibit lesions in mouse models of atherosclerosis), compared with the nonoxidized phospholipids, were dramatically increased. Interestingly, the binding of oxidized and nonoxidized FFAs to the 4F peptides was of equally high affinity, with K_D values ranging between 10^{-5} and 10^{-10} M (Table 2). Thus, the binding affinity of the phospholipids for the 4F peptides only approached that of the FAs after the phospholipids were oxidized.

As noted above, in the case of apoA-I, the binding of phospholipids was similar whether oxidized or not oxidized. However, the binding of the FFAs (arachidonic and linoleic acids) to apoA-I decreased dramatically when they were oxidized (Table 2).

Epand et al. (9) studied the interaction of L-4F with a synthetic membrane containing phospholipid with and without cholesterol. They found that the peptide penetrated more deeply into the membrane in the absence of cholesterol and in the presence of cholesterol, resulted in the separation of cholesterol from the phospholipid. These results might suggest a higher binding affinity of L-4F for the phospholipid, compared with the cholesterol. As shown in Fig. 2, before oxidation, the apparent K_D (K_{Dapp}) value for the binding of the phospholipid to the 4F peptides was $\sim 10^{-4}$ M. As shown in Table 3 the K_D value for the binding of cholesterol to the 4F peptides was $\sim 10^{-7}$ M. These differences may be due to several factors: *i*) differences in the phospholipids studied (SOPC in the case of Epand et al. and PAPC here); *ii*) the mechanism promoting the separation of cholesterol from the membrane phospholipid may not be related to differences in the binding affinities; or *iii*) the differences in studying these interactions in a membrane versus studying the interactions in a nonmembrane environment.

Both oxidized phospholipids and oxidized FAs bound with much higher affinity to the peptides than to apoA-I (Tables 1 and 2). Interestingly, the binding affinity of oxidized phospholipids for the peptides was even higher than the binding affinity of the oxidized FAs for the peptides (Tables 1 and 2). Differences in relative polarity or differences in tertiary structure between the two classes of oxidized lipids may have contributed to these differences in binding affinity for the peptides.

The results reported here cannot be attributable to the amine-coupling procedure used to attach the peptides to the biosensor chip surface. The remarkably high affinity of the 4F mimetic peptides for oxidized phospholipids was seen both when L-4F was immobilized to the sensor chip by a biotin-streptavidin linkage and the phospholipids were in solution (Fig. 4) and when biotinylated phospholipids were immobilized on the sensor chip and the 4F peptides remained in solution (Fig. 5).

The activity of class A amphipathic helical peptides in biological systems was suggested to depend on hydrophobic face-lipid acyl chain interactions (10, 29, 36). Based on the imputed molecular shapes of 3F-2 and $3F^{14}$, it was predicted that the entry of water and oxidized lipids into the surrounding hydrophobic milieu of the peptide would be favored for the 3F-2 molecule but not for $3F^{14}$ (29). Similar considerations may explain why the apoA-I-mimetic peptide

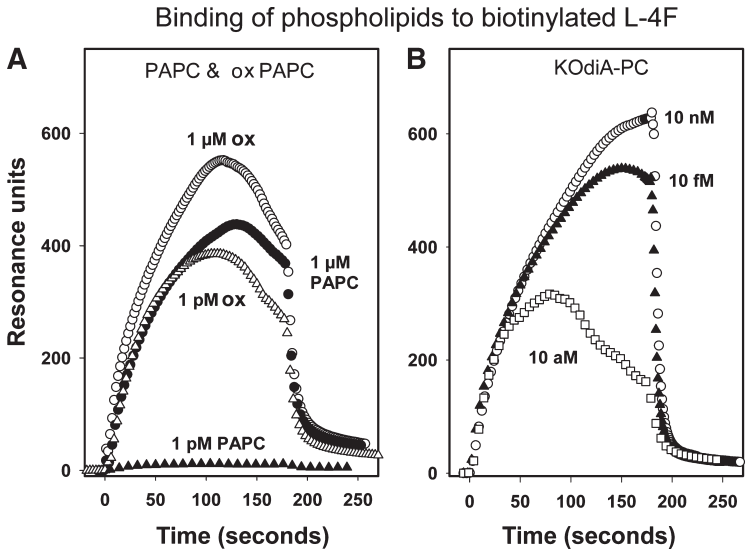

Fig. 4. Binding to biotinylated L-4F. A: The binding of native PAPC and PAPC subjected to 24 h of oxidation (oxPAPC) compared to biotinylated L-4F. The biotinylated peptide (1,213 RUs) was immobilized via streptavidin to a CM5 biosensor chip. B: Binding of KOdiA-PC to the same biosensor.

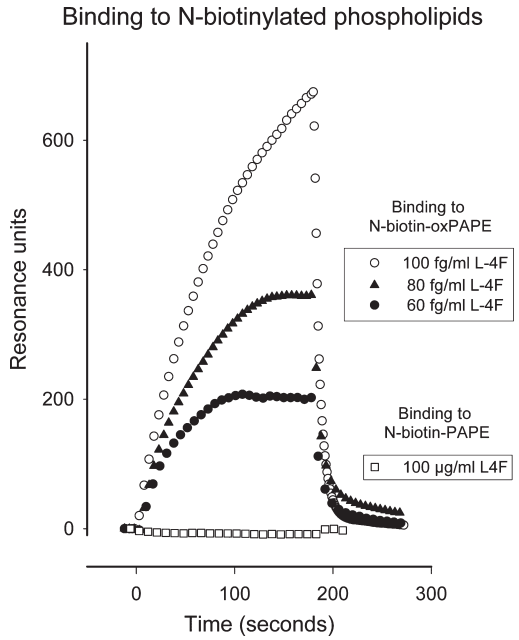

Fig. 5. Binding of L-4F to N-biotinylated phospholipids. N-biotinylated-PAPE and N-biotinylated-oxPAPE were immobilized on BIAcore SA sensor chips precoated with streptavidin, and used to detect the binding by L-4F in solution. L-4F binding to PAPE-*N*-Biotin was measured over a wide concentration range (100 fg/ml to 1 mg/ml), with results similar to those shown for 100 µg/ml.

4F inhibits lesion formation in mouse models of atherosclerosis, whereas 2F (another class A amphipathic helical peptide) does not (36). Consistent with the present data, the mimetic peptides 3F-2 and 4F removed lipid hydroperoxides from the LDL of Watanabe rabbits, whereas $3F^{14}$ did not (10). 3F-2 and 4F also prevented oxPAPC from inducing MCP-1 activity in cocultured human aortic endothelial and smooth muscle cells, whereas $3F^{14}$ did not (10).

The enhanced binding of the 4F peptides has been attributed to their ability to interact with lipid membranes, creating microdomains for the sequestration of polar lipids derived from an aqueous environment (36). In the experiments utilizing sensor chips, this mechanism would not be operative. However, it is possible and, we think, likely that microdomains in the water layer surrounding the immobilized peptides provide a similar thermodynamically favored environment for oxidized lipids. We believe that the structural basis of the binding of oxidized lipids to the peptides relates to the fact that the oxidized lipids are more polar than the nonoxidized lipids from which they are derived and the peptides provide a microenvironment that thermodynamically is more favorable than either the pure lipid or the aqueous environment in which they were formed.

Recently Wool, Reardon, and Getz (37) reported in vitro studies showing that dimers of the 4F peptide linked by proline or alanine or the sequence KVEPLRA produced more remodeling of HDL and more cholesterol efflux compared with 4F alone. However, 4F alone was more effective in preventing LDL oxidation than was the case for the dimers. The physiologic relevance of the differences in the affinities of apoA-I and apoA-I-mimetic peptides will be determined in vivo by the amounts or fluxes of the oxidized lipids and the amounts or fluxes of peptide versus apoA-I in the plasma at a steady state. The concentration of cholesterol in the plasma of apoE-null mice is measured in the range of mg/ml. The concentration of oxidized phospholipids in the plasma of apoE-null mice is measured in the range of µg/ml (38). The four to six orders of magnitude difference in the affinity of the apoA-I-mimetic peptides for binding these oxidized phospholipids compared with apoA-I (Table 1) appears sufficient to favor the peptides over apoA-I, as shown by the experiment in presented in Fig. 1.

Recently, we demonstrated that feeding a Western diet to LDL receptor-null mice caused an accumulation of oxidized phospholipids in the kidneys associated with renal inflammation. Consistent with in vitro studies indicating that oxPAPC induces cytokine production through a sterol-regulatory element binding protein (SREBP)-mediated mechanism (39, 40), renal SREBP-1c mRNA levels increased dramatically in mice fed the Western diet, compared with

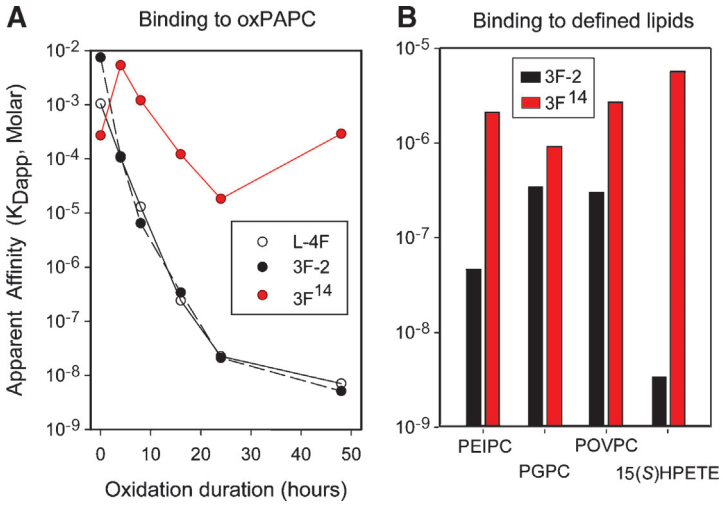

Fig. 6. Binding of oxidized PAPC to immobilized $3F^{14}$ versus 3F-2. A: The apparent K_D (K_{Dapp}) of oxPAPC to $3F^{14}$ (red circle), 3F-2 (solid black circle) and for comparison, L-4F (open black circle) as described in Materials and Methods. The PAPC was air-oxidized for 0–48 h, as indicated. K_{Dapp} values were determined at six time points. B: K_D values for four defined oxidized lipids, PEIPC (1-palmitoyl-2-(5,6-eoxyisoprostane E2)-*sn*-glycero-3-phosphorylcholine); PGPC (1-palmitoyl-2-glutaroyl-*sn*-glycero-3-phosphorylcholine); POVPC, (1-palmitoyl-2-(5-oxovaleroyl)-*sn*-glycero-3-phosphorylcholine), and 15(*S*)-HPETE (hydroperoxyeicosatetraenoic acid). Note that the taller the bar (higher K_D value), the lower the binding affinity.

the same mice on a chow diet (22). The increased SREBP-1c mRNA levels were associated with a significant increase in renal triglyceride levels. Adding D-4F to the drinking water of the LDL receptor-null mice on the Western diet did not alter plasma triglycerides, cholesterol, or LDL + VLDL cholesterol levels, nor did it significantly change renal cholesterol levels. However, the addition of D-4F to the drinking water reduced the levels of oxidized phospholipids in the kidneys to those seen in mice on chow and similarly reduced SREBP-1c mRNA levels and renal triglyceride levels without altering the levels of apoB retained in the kidneys. Thus, the action of the apoA-I-mimetic peptide appeared to be specifically related to the levels and known mechanisms of action of oxPAPC in inducing inflammatory cytokines (22).

Because the maximum plasma levels of D-4F achieved in mice after oral administration are only about ~130 nM (7), and plasma levels of apoA-I in mice are ~35 μM, it has been difficult to understand how 4F might achieve its beneficial effects in vivo. The dramatic difference in binding affinities for oxidized phospholipids between the mimetic peptides and apoA-I could explain how these apoA-I-mimetic peptides exert their potent biological activities, even when surrounded by a "sea" of apoA-I. The results of the experiments shown in Fig. 1, where concentrations of full-length human apoA-I were similar to those in plasma and did not inhibit LDL-induced monocyte chemotactic activity, but the addition of 4.3 nM of L-4F significantly reduced this activity and 0.43 μM was as effective as normal human HDL, are consistent with this explanation.

We previously reported that the peptide $3F^{14}$ was unable to inhibit LDL-induced monocyte chemotactic activity, in contrast to the potent inhibition seen with L-4F (see Fig. 5 in Ref. 1). The binding data reported here (Fig. 6), coupled with the data previously reported on $3F^{14}$ (see Fig. 5 in Ref. 1; see Ref. 30 for studies in a mouse model of atherosclerosis), suggest that a strategy seeking to design anti-inflammatory apoA-I-mimetic peptides should not focus on the binding properties of the peptides for *nonoxidized* lipids, but rather should focus on developing peptides that bind *oxidized* lipids with very high affinity.

REFERENCES

1. Datta, G., M. Chaddha, S. Hama, M. Navab, A. M. Fogelman, D. W. Garber, V. K. Mishra, R. M. Epand, R. F. Epand, S. Lund-Katz, et al. 2001. Effects of increasing hydrophobicity on the physical-chemical and biological properties of class A amphipathic helical peptide. *J. Lipid Res.* **42:** 1096–1104.
2. Navab, M., G. M. Anantharamaiah, S. Hama, D. W. Garber, M. Chaddha, G. Hough, R. Lallone, and A. M. Fogelman. 2002. Oral administration of an apoA-I mimetic peptide synthesized from D-amino acids dramatically reduces atherosclerosis in mice independent of plasma cholesterol. *Circulation.* **105:** 290–292.
3. Van Lenten, B. J., A. C. Wagner, G. M. Anantharamaiah, D. W. Garber, M. C. Fishbein, L. Adhikary, D. P. Nayak, S. Hama, M. Navab, and A. M. Fogelman. 2002. Influenza infection promotes macrophage traffic into arteries of mice that is prevented by D-4F, an apolipoprotein A-I mimetic peptide. *Circulation.* **106:** 1127–1132.
4. Ou, Z., J. Ou, A. W. Ackerman, K. T. Oldham, and K. A. Pritchard, Jr. 2003. L-4F, an apolipoprotein A-1 mimetic, restores nitric oxide and superoxide anion balance in low-density lipoprotein-treated endothelial cells. *Circulation.* **107:** 1520–1524.
5. Ou, J., Z. Ou, D. W. Jones, S. Holzhauer, O. A. Hatoum, A. W. Ackerman, D. W. Weihrauch, D. D. Gutterman, K. Guice, K. T. Oldham, et al. 2003. L-4F, an apolipoprotein A-I mimetic, dramatically improves vasodilation in hypercholesterolemia and sickle cell disease. *Circulation.* **107:** 2337–2341.
6. Van Lenten, B. J., A. C. Wagner, M. Navab, G. M. Anantharamaiah, E. K. Hui, D. P. Nayak, and A. M. Fogelman. 2004. D-4F, an apolipoprotein A-I mimetic peptide, inhibits the inflammatory response induced by influenza A infection of human type II pneumocytes. *Circulation.* **110:** 3252–3258.
7. Navab, M., G. M. Anantharamaiah, S. T. Reddy, S. Hama, G. Hough, V. R. Grijalva, A. C. Wagner, J. S. Frank, G. Datta, D. Garber, and A. M. Fogelman. 2004. Oral D-4F causes formation of pre-β high-density lipoprotein and improves high-density lipoprotein-mediated cholesterol efflux and reverse cholesterol transport from macrophages in apolipoprotein E-null mice. *Circulation.* **109:** 3215–3220.
8. Li, X., K-Y. Chyu, J. R. F. Neto, J. Yano, N. Nathwani, C. Ferreira, P. C. Dimayuga, B. Cercek, S. Kaul, and P. K. Shah. 2004. Differential effects of apolipoprotein A-I mimetic peptide on evolving and established atherosclerosis in apolipoprotein E-null mice. *Circulation.* **110:** 1701–1705.
9. Epand, R. M., R. F. Epand, B. G. Sayer, G. Melacini, M. N. Palgunachari, J. P. Segrest, and G. M. Anantharamaiah. 2004. An apolipoprotein AI mimetic peptide: membrane interactions and the role of cholesterol. *Biochemistry.* **43:** 5073–5083.
10. Datta, G., R. F. Epand, R. M. Epand, M. Chaddha, M. A. Kirksey, D. W. Garber, S. Lund-Katz, M. C. Phillips, S. Hama, M. Navab, et al. 2004. Aromatic residue position on the nonpolar face of class A amiphipathic helical peptides determines biological activity. *J. Biol. Chem.* **279:** 26509–26517.
11. Navab, M., G. M. Anantharamaiah, S. Hama, G. Hough, S. T. Reddy, J. S. Frank, D. W. Garber, S. Handattu, and A. M. Fogelman. 2005. D-4F and statins synergize to render HDL anti-inflammatory in mice and monkeys and cause lesion regression in old apolipoprotein E-null mice. *Arterioscler. Thromb. Vasc. Biol.* **25:** 1426–1432.
12. Ou, J., J. Wang, H. Xu, Z. Ou, M. G. Sorci-Thomas, D. W. Jones, P. Signorino, J. C. Densmore, S. Kaul, K. T. Oldham, et al. 2005. Effects of D-4F on vasodilation and vessel wall thickness in hypercholesterolemic LDL receptor-null and LDL receptor/apolipoprotein A-I double-knock out mice on Western diet. *Circ. Res.* **97:** 1190–1197.
13. Kruger, A. L., S. Peterson, S. Turkseven, P. M. Kaminski, F. F. Zhang, S. Quan, M. S. Wolin, and N. G. Abraham. 2005. D-4F induces heme oxygenase-1 and extracellular superoxide dismutase, decreases endothelial cell sloughing, and improves vascular reactivity in rat model of diabetes. *Circulation.* **111:** 3126–3134.
14. Gupta, H., L. Dai, G. Datta, D. W. Garber, H. Grenett, Y. Li, V. Mishra, M. N. Palgunachari, S. Handattu, S. H. Gianturco, et al. 2005. Inhibition of lipopolysaccharide-induced inflammatory responses by an apolipoprotein AI mimetic peptide. *Circ. Res.* **97:** 236–243.
15. Tang, C., A. M. Vaughan, G. M. Anantharamaiah, and J. F. Oram. 2006. Janus kinase 2 modulates the lipid-removing but not protein stabilizing interactions of amphipathic helices with ABCA1. *J. Lipid Res.* **47:** 107–114.
16. Schnickel, G. T., G. R. Hsieh, E. L. Kachikwu, C. Garcia, A. Shefizadeh, M. C. Fishbein, and A. Ardehali. 2006. Cytoprotective gene HO-1 and chronic rejection in heart transplantation. *Transplant. Proc.* **38:** 3259–3262.
17. Buga, G. M., J. S. Frank, G. A. Mottino, M. Hendizadeh, A. Hakhamian, J. H. Tillisch, S. T. Reddy, M. Navab, G. M. Anantharamaiah, L. J. Ignarro, et al. 2006. D-4F decreases brain arteriole inflammation and improves cognitive performance in LDL receptor-null mice on a Western diet. *J. Lipid Res.* **47:** 2148–2160.
18. Peterson, S. J., D. Husney, A. L. Kruger, R. Olszanecki, F. Ricci, L. F. Rodella, A. Stacchiotti, R. Rezzani, J. A. McClung, W. S. Aronow, et al. 2007. Long-term treatment with the apolipoprotein A1 mimetic peptide increases antioxidants and vascular repair in type I diabetic rats. *J. Pharmacol. Exp. Ther.* **322:** 514–520.
19. Hsieh, G. R., G. T. Schnickel, C. Garcia, A. Shefizadeh, M. C. Fishbein, and A. Ardehali. 2007. Inflammation/oxidation in chronic rejection: apolipoprotein A-I mimetic peptide reduces chronic rejection of transplanted hearts. *Transplantation.* **84:** 238–243.
20. Weihrauch, D., H. Xu, Y. Shi, J. Wang, J. Brien, D. W. Jones, S. Kaul, R. A. Komorowski, M. E. Csuka, K. T. Oldham, et al. 2007. Effects of D-4F on vasodilation, oxidative stress, angiostatin, myocardial inflammation, and angiogenic potential in tight-skin mice. *Am. J. Physiol. Heart Circ. Physiol.* **293:** H1432–H1441.
21. Van Lenten, B. J., A. C. Wagner, M. Navab, G. M. Anantharamaiah,

S. Hama, S. T. Reddy, and A. M. Fogelman. 2007. Lipoprotein inflammatory properties and serum amyloid A levels but not cholesterol levels predict lesion area in cholesterol-fed rabbits. *J. Lipid Res.* **48:** 2344–2353.
22. Buga, G. M., J. S. Frank, G. A. Mottino, A. Hakhamian, A. Narasimha, A. D. Watson, B. Yekta, M. Navab, S. T. Reddy, G. M. Anantharamaiah, et al. 2008. D-4F reduces EO6 immunoreactivity, SREBP-1c mRNA levels, and renal inflammation in LDL receptor-null mice fed a Western diet. *J. Lipid Res.* **49:** 192–205.
23. Bloedon, L. T., R. L. Dunbar, D. Duffy, P. Pinell-Salles, R. Norris, B. J. DeGroot, R. Movva, M. Navab, A. M. Fogelman, and D. J. Rader. 2008. Safety, pharmacokinetics, and pharmacodynamics of oral apoA-I mimetic peptide D-4F in high-risk cardiovascular patients. *J. Lipid Res.* **49:** 1344–1352.
24. Navab, M., G. M. Anantharamaiah, S. T. Reddy, S. Hama, G. Hough, V. R. Grijalva, N. Yu, B. J. Ansell, G. Datta, D. W. Garber, et al. 2005. Apolipoprotein A-I mimetic peptides. *Arterioscler. Thromb. Vasc. Biol.* **25:** 1325–1331.
25. Navab, M., S. Y. Hama, G. M. Anantharamaiah, K. Hassan, G. P. Hough, A. D. Watson, S. T. Reddy, A. Sevanian, G. C. Fonarow, and A. M. Fogelman. 2000. Normal high density lipoprotein inhibits three steps in the formation of mildly oxidized low density lipoprotein: steps 2 and 3. *J. Lipid Res.* **41:** 1495–1508.
26. Podrez, E. A., E. Poliakov, Z. Shen, R. Zhang, Y. Deng, M. Sun, P. J. Finton, L. Shan, M. Febbraio, D. P. Hajjar, et al. 2002. A novel family of atherogenic oxidized phospholipids promotes macrophage foam cell formation via the scavenger receptor CD36 and is enriched in atherosclerotic lesions. *J. Biol. Chem.* **277:** 38517–38523.
27. Gharavi, N. M., P. S. Gargalovic, I. Chang, J. A. Araujo, M. J. Clark, W. L. Szeto, A. D. Watson, A. J. Lusis, and J. A. Berliner. 2007. High-density lipoprotein modulates oxidized phospholipid signaling in human endothelial cells from proinflammatory to anti-inflammatory. *Arterioscler. Thromb. Vasc. Biol.* **27:** 1346–1353.
28. Subbanagounder, G., J. W. Wong, H. Lee, K. F. Faull, E. Miller, J. L. Witztum, and J. A. Berliner. 2002. Epoxyisoprostane and epoxycyclopentenne phospholipids regulate monocyte chemotactic protein-1 and interleukin-8 synthesis. Formation of these oxidized phospholipids in response to interleukin-1β. *J. Biol. Chem.* **277:** 7271–7281.
29. Epand, R. M., R. F. Epand, B. G. Sayer, G. Datta, M. Chaddha, and G. M. Anantharamaiah. 2004. Two homologus apolipoprotein AI mimetic peptides. Relationship between membrane interactions and biological activity. *J. Biol. Chem.* **279:** 51404–51414.
30. Handattu, S. P., D. W. Garber, D. C. Horn, D. W. Hughes, B. Berno, A. D. Bain, V. K. Mishra, M. N. Palgunachari, G. Datta, G. M. Anantharamaiah, et al. 2007. ApoA-I mimetic peptides with differing ability to inhibit atherosclerosis also exhibit differences in their interactions with membrane bilayers. *J. Biol. Chem.* **282:** 1980–1988.
31. Fields, G. B., and R. L. Noble. 1990. Solid phase peptide synthesis utilizing 9-fluorenylmethoxycarbonyl amino acids. *Int. J. Pept. Protein Res.* **35:** 161–214.
32. Watson, A. D., N. Leitinger, M. Navab, K. F. Faull, H. Sohvi, J. L. Witztum, W. Palinski, D. Schwenke, R. G. Salomon, W. Sha, et al. 1997. Structural identification by mass spectrometry of oxidized phospholipids in minimally oxidized low density lipoprotein that induce monocyte/endothelial interactions and evidence for their presence in vivo. *J. Biol. Chem.* **272:** 13597–13607.
33. Watson, A. D., G. Subbanagounder, K. F. Faull, M. Navab, M. E. Jung, A. M. Fogelman, and J. A. Berliner. 1999. Structural identification of a novel pro-inflammatory epoxyisoprostane phospholipid in mildly oxidized low density lipoprotein. *J. Biol. Chem.* **274:** 24787–24798.
34. Gugiu, B. G., K. Mouillesseaux, V. Duong, T. Herzog, A. Hekimian, L. Koroniak, T. M. Vondriska, and A. D. Watson. 2008. Protein targets of oxidized phospholipids in endothelial cells. *J. Lipid Res.* **49:** 510–520.
35. Garber, D. W., G. Datta, M. Chaddha, M. N. Palgunachari, S. Y. Hama, M. Navab, A. M. Fogelman, J. P. Segrest, and G. M. Anantharamaiah. 2001. A new synthetic class A amphipathic peptide analogue protects mice from diet-induced atherosclerosis. *J. Lipid Res.* **42:** 545–552.
36. Anantharamaiah, G. M., V. K. Mishra, D. W. Garber, G. Datta, S. P. Handattu, M. N. Palgunachari, M. Chaddha, M. Navab, S. T. Reddy, J. P. Segrest, et al. 2007. Structural requirements for anti-oxidative and anti-inflammatory properties of apolipoprotein A-I mimetic peptides. *J. Lipid Res.* **48:** 1915–1923.
37. Wool, G. D., C. A. Reardon, and G. S. Getz. 2008. Apolipoprotein A-I mimetic peptide helix number and helix linker influence potentially anti-atherogenic properties. *J. Lipid Res.* **49:** 1268–1283.
38. Forte, T. M., G. Subbanagounder, J. A. Berliner, P. J. Blanche, A. O. Clermont, Z. Jia, M. N. Oda, R. M. Krauss, and J. K. Bielicki. 2002. Altered activities of anti-atherogenic enzymes LCAT, paraoxonase, and platelet-activating factor acetylhydrolase in atherosclerosis-susceptible mice. *J. Lipid Res.* **43:** 477–485.
39. Yeh, M., A. L. Cole, J. Choi, Y. Liu, D. Tulchinsky, J. H. Qiao, M. C. Fishbein, A. N. Dooley, T. Hovnanian, K. Mouilleseaux, et al. 2004. Role for sterol regulatory element-binding protein in activation of endothelial cells by phospholipid oxidation products. *Circ. Res.* **95:** 780–788.
40. Gharavi, N. M., N. A. Baker, K. P. Mouillesseaux, W. Yeung, H. M. Honda, X. Hsieh, M. Yeh, E. J. Smart, and J. A. Berliner. 2006. Role of endothelial nitric oxide synthase in the regulation of SREBP activation by oxidized phospholipids. *Circ. Res.* **98:** 768–776.

ERRATA

The authors of "Anti-inflammatory apoA-I-mimetic peptides bind oxidized lipids with much higher affinity than human apoA-I" (*J. Lipid Res.* 2008 49: 2302–2311) would like to disclose the following information:

MN, SH, GMA and AMF are principals in Bruin Pharma and AMF is an officer in Bruin Pharma.

This information was omitted from the online article but has since been added.

DOI 10.1194/jlr.ERRM800075-JLR